

X-ray induces mechanical and heat allodynia in mouse via TRPA1 and TRPV1 activation

Molecular Pain
Volume 15: 1–13
© The Author(s) 2019
Article reuse guidelines:
sagepub.com/journals-permissions
DOI: 10.1177/1744806919849201
journals.sagepub.com/home/mpx



Su Cun-Jin^{1,2} , Xu Jian-Hao³, Liu Xu², Zhao Feng-Lun¹, Pan Jie¹, Shi Ai-Ming¹, Hu Duan-Min⁴, Yu Yun-Li⁵, Liu Tong^{2,6}, and Zhang Yu-Song³

Abstract

Radiotherapy-related pain is a common adverse reaction with a high incidence among cancer patients undergoing radiotherapy and remarkably reduces the quality of life. However, the mechanisms of ionizing radiation-induced pain are largely unknown. In this study, mice were treated with 20 Gy X-ray to establish ionizing radiation-induced pain model. X-ray evoked a prolonged mechanical, heat, and cold allodynia in mice. Transient receptor potential vanilloid 1 and transient receptor potential ankyrin 1 were significantly upregulated in lumbar dorsal root ganglion. The mechanical and heat allodynia could be transiently reverted by intrathecal injection of transient receptor potential vanilloid 1 antagonist capsazepine and transient receptor potential ankyrin 1 antagonist HC-030031. Additionally, the phosphorylated extracellular regulated protein kinases (ERK) and Jun NH2-terminal Kinase (JNK) in pain neural pathway were induced by X-ray treatment. Our findings indicated that activation of transient receptor potential ankyrin 1 and transient receptor potential vanilloid 1 is essential for the development of X-ray-induced allodynia. Furthermore, our findings suggest that targeting on transient receptor potential vanilloid 1 and transient receptor potential ankyrin 1 may be promising prevention strategies for X-ray-induced allodynia in clinical practice.

Keywords

X-ray, radiation, pain, transient receptor potential vanilloid 1, transient receptor potential ankyrin 1, dorsal root ganglion

Date Received: 18 March 2019; revised: 10 April 2019; accepted: 15 April 2019

Introduction

Ionizing radiation (IR) therapy is still a cornerstone of modern cancer treatment,¹ with an approximately half of newly diagnosed cancer patients receiving radiotherapy at some point in the course of the disease.^{2,3} However, radiotherapy is associated with a risk of various side effects, including nausea, vomiting,⁴ enteropathy, and lung injury.⁵ Skin is the largest organ and is the biological defense barrier at any irradiated area. Skin injury is another common side effect after radiation treatment.^{6,7} Radiation may cause variety of physical skin reactions and contributes to pain, itch, and burning.⁸ A moderate-to-severe skin reaction occurs in about 85% of patients treated with radiotherapy.^{9,10} The IR-induced skin changes can affect daily living activities and life quality.¹¹

¹Department of Pharmacy, The Second Affiliated Hospital of Soochow University, Suzhou, China

²Institute of Neuroscience, Soochow University, Suzhou, China

³Department of Oncology, The Second Affiliated Hospital of Soochow University, Suzhou, China

⁴Department of Gastroenterology, The Second Affiliated Hospital of Soochow University, Suzhou, China

⁵Department of Clinical Pharmacology, The Second Affiliated Hospital of Soochow University, Suzhou, China

⁶College of Life Sciences, Yanan University, Yanan, China

The first three authors contributed equally to this work.

Corresponding Author:

Zhang Yu-Song, Department of Oncology, The Second Affiliated Hospital of Soochow University, Suzhou, China.

Email: zhangyusong19@163.com



Similar to chemotherapy-induced peripheral neuropathy pain,^{12,13} a sensory adverse event is common at the site of skin after radiation treatment. However, the underlying mechanisms of IR-induced allodynia are poorly understood. Several members within the transient receptor potential (TRP) channel family act as the sensors for temperature and noxious stimuli and are involved in the development of pathological pain.¹⁴ Transient receptor potential ankyrin 1 (TRPA1) and transient receptor potential vanilloid 1 (TRPV1) are co-expressed in a specific subgroup of dorsal root ganglion (DRG) neurons that contributes to the detection and transduction of noxious stimuli.^{15,16} TRPA1 is sensitive to endogenous reactive molecules, which are produced at the damaged tissue sites, including reactive oxygen species (ROS) and reactive nitrogen species (RNS).^{17–20} TRPV1 is expressed in about 60% of peptidergic small neurons in DRG and trigeminal ganglia. TRPV1 can be activated under inflammation condition.²¹ Genetic and pharmacological studies have reported that TRPV1 contributes to chronic inflammatory pain and neuropathic pain.^{22,23}

In this study, we investigated the roles of TRP channels in a mouse pain model induced by X-ray, which is commonly used in radiotherapy. Biochemical and pharmacologic experiments indicate that TRPA1 and TRPV1, but not TRPV4, are necessary for the development of X-ray-induced mechanical and heat allodynia in mice. These findings will be helpful in prevention and treatment of pain after radiotherapy.

Materials and methods

Animal

Adult male C57BL/6 mice (25–30 g) were obtained from the SLAC Laboratory Animal Co., Ltd. (Shanghai, China). Four mice were housed per cage, with food and water available ad libitum. All mice were kept in controlled room temperature ($22 \pm 2^\circ\text{C}$) and humidity (60%–80%). The illumination maintained on a 12 h/12 h light/dark cycle (lights on from 6:00 a.m. to 6:00 p.m.). The animal study was approved by the University Committee on Animal Care of Soochow University (No. 2012–03) and conducted in accordance with the guidelines of Animal Use and Care of the Jiangsu Province (2008).

Reagents

HC-030031, TRPA1, and TRPV4 inhibitors were purchased from MedChemExpress (MCE). TRPA1 and TRPV1 antibodies were purchased from Alomone, TRPV4 antibody was purchased from Abcam, pERK and pJNK antibodies were purchased from CST, and

glyceraldehyde 3-phosphate dehydrogenase (GAPDH) antibody was purchased from Affinity. IB4 was purchased from Thermo Fisher. The detailed information is shown in Supplementary Data Table 1.

X-ray-induced allodynia model

Although there are several studies in radiation-induced skin injury, the studies about IR-induced pain are rarely reported. In this study, mice were anesthetized with an intraperitoneal (i.p.) injection of chloral hydrate (300 mg/kg). Mice were immobilized with adhesive tape on a plastic plate to minimize motion during irradiation exposure. A 3-cm thick piece of lead was used to localize the radiation field and protect other fields. In the first series of experiments, a single dose of 10 Gy or 20 Gy X-ray was administered to the right hind limbs (Supplementary Data Figure 1) at a dose rate of 2 Gy/min using RAD SOURCE RS2000 X-ray machine (160 kVp, GA, USA). In the second series of experiments, a single dose of 20 Gy was administered to the hind limbs and tails at a dose rate of 2 Gy/min (Supplementary Data Figure 2). After irradiation, the mice were fed normally. Painful behavior tests were performed in the following days.

Intrathecal injection

Mice were under a brief anesthesia with isoflurane, then we delivered drugs into cerebral spinal fluid (CSF) space around lumbosacral spinal cord through intrathecal (i.t.) injection. Spinal cord puncture was made with a 30 G needle between the lumbar L5 and L6 to inject the TRP channels inhibitors (10 μg in 10 μl) to the CSF.^{24,25} A brisk tail-flick after the needle entry into subarachnoid space signed a successful spinal puncture.

Behavioral tests

Behavioral tests were assessed in a quiet and temperature controlled room between 9 a.m. and 5 p.m. and were carried out by an operator blinded to the genotypes and drug treatments.

Mechanical allodynia. Mechanical allodynia was assessed using the “up-and-down” methods as previously described.²⁶ Mice were placed beneath perspex boxes (10 \times 10 \times 7 cm) set upon elevated wire mesh stands and acclimated for 30 min. Von Frey filament (0.008–1.4 g) was applied to the mid-plantar area with enough pressure to bend the hair. The filament was held for 5 s. If the paw did not lift after 5 s, an increased weight filament would be used next. Whereas a subsequently weaker filament would be used if the paw lifted after filament stimuli. The 50% mechanical paw withdrawal threshold was collected as described previously.²⁶ The

paw mechanical withdraw thresholds were recorded in grams, and they were detected before (baseline), 1 to 40 days after IR treatment, and after drug treatments (2, 5, 12, and 24 h).

Heat allodynia. The heat hyperalgesia was measured using hot-plate test and tail-flick test. Hot-plate test was conducted by placing mice on a hot plate at 55°C. Behaviors, including paw licking, stomping, jumping, and escaping from the hot plate, were considered as positive responses, and the latency was recorded. The cut off time for the hot-plate test was 15 s. Tail-flick test was carried out by immersing the mouse tail in water (5 cm from the tip) maintained at 48°C temperature. Tail-flick latency time was measured as the time from the heat exposure to the withdrawal time of the tail. The cut off time for tail-flick test was 15 s. This test was carried out three times per mouse, and the average value was taken as latency time.

Cold behavioral test. Cold hyperalgesia was analyzed by the acetone stimulation test. Mice were placed into perspex boxes (10 × 10 × 7 cm) with a wire mesh floor. Mice were allowed to habituate for 30 min prior to the test. A drop (0.05 ml) of acetone was placed onto the center of planta skin. The responses to acetone were recorded 30 s after acetone application. Responses to acetone are divided into 4 grades: 0, no response; 1, quick withdraw, flick or stamp of the paw; 2, prolonged withdraw or repeat flicking of the paw; and 3, repeated flicking of the paw with licking directed at the ventral side of the paw. Acetone was applied to each paw three times at 10- to 15-min intervals, and the average score was calculated.

RNA isolation and quantitative real-time polymerase chain reaction

Total RNA was extracted using Trizol Reagent (Invitrogen, Carlsbad, California) according to the protocol. Total RNA (1 µg) was used to synthesize cDNA by reverse transcription using Revert Aid First Strand cDNA Synthesis Kit (Thermo Fisher Scientific, Waltham, USA). Quantitative real-time polymerase chain reaction (qPCR) test was conducted by SYBR Green PCR Master Mix (Roche, Basel, Switzerland) using real-time PCR Detection System (ABI 7500, Life technology, USA). The cycling conditions included a 10-min initial denaturation step at 95°C followed by 40 cycles of 15 s at 95°C and 1 min at 60°C. Target gene expression was normalized to the housekeeper gene GAPDH expression. Relative fold difference in expression was calculated using $2^{-\Delta\Delta C_t}$ method after normalization to GAPDH expression. The primers (Genewiz) are shown in Supplementary Data Table 2.

Protein extraction and Western blot analysis

Hind paw skin, sciatic nerve (SN), and DRGs (L2–L5) were collected from mice treated with radiation at different time points. Tissue samples were homogenized in radioimmunoprecipitation assay (Beyotime Biotechnology, China) lysis buffer containing protease and phosphatase inhibitors (Roche). Protein concentration was determined using bicinchoninic acid assay (Beyotime Biotechnology, China). Protein (40 µg) in each sample was separated by 10% sodium dodecyl sulfate-polyacrylamide gel electrophoresis gel. The protein was transferred to the polyvinylidene fluoride membrane (Millipore). Blots were blocked for 1 h with 5% skim milk at room temperature and incubated with primary antibodies (TRPA1, Alomone; TRPV1, Alomone; TRPV4, Millipore; pERK and pJNK, CST; GAPDH, Affinity, the detailed information is shown in Supplementary Data Table 1) at 4°C overnight. Blots were washed with TBST (25 mM Tris-HCl, 150 mM NaCl, 0.1% Tween-20, pH 7.6) three times and incubated with secondary antibodies for 1 h at room temperature. The protein bands were detected using enhanced chemiluminescence solution (Pierce, Thermo Scientific). The density of target bands was analyzed using ImageJ software (Wayne Rasband). The GAPDH bands were used as control for normalization.

Histology and immunofluorescence

Mice were anesthetized using chloral hydrate (400 mg/kg, i.p.) and perfused with physiological saline transcardially, followed by 4% paraformaldehyde at different time points after radiation treatment. Paraffin sections of paw skin (10 µm) were stained with hematoxylin and eosin (H&E) for histological examination. Cryosections (15 µm) of DRGs (L2–L5) were incubated with the primary antibody rabbit anti-TRPA1 and IB4 (Alexa Fluor 488 Conjugate) or rabbit anti-TRPV1 and IB4 diluted in 5% bovine serum albumin-PBST (137 mM NaCl, 2.7 mM KCl, 10 mM Na₂HPO₄, and 1.5 mM KH₂PO₄, pH 7.4 and 0.1% Tween 20) overnight at 4°C. Sections were then incubated with fluorescent secondary antibodies. Sections were captured using Leica fluorescence microscope.

Statistical analysis

Data were analyzed using Graph Prism 6 (Graph Pad, La Jolla, CA). All data were expressed as mean ± S.E.M. Student's t test was used for two-group comparisons. One-way or two-way analysis of variance followed by the post hoc Bonferroni's test was used for multiple comparisons. The criterion for statistical significance was $p < 0.05$.

Results

Establishment of ionizing radiation-induced allodynia model in mice

In the first series of experiments, we explored whether a single treatment of X-ray radiation could induce pain-like behavior. The right hind limb of mouse was treated with a single dose of 10 Gy or 20 Gy X-ray using RAD SOURCE RS2000 X-ray machine (Supplementary Data Figure 1(A)). The mechanical allodynia was assessed using Von Frey hairs. Reduced mechanical threshold was observed as early as 24 h (Figure 1(a); $F(2, 22) = 12.86$, $p < 0.05$) and lasted eight days at least after X-ray treatment (Figure 1(a); $F(2, 22) = 62.279$, $p < 0.001$). There was no significant difference of the mechanical threshold between 10 Gy and 20 Gy. In addition, the mechanical threshold of the left hind limb, which was not exposed to X-ray, was similar to control mice

(Supplementary Data Figure 1(B)). This indicated that X-ray-induced allodynia was local and did not affect contralateral pain perception. There was no obvious change in the morphology of skin tissue at 14 days after radiation using H&E staining (Figure 1(b)). This eliminated the painful behavior secondary to skin ulceration and indicated that the allodynia was specific to radiation.

In the following experiments, double hind limbs and tail of mouse (Supplementary Data Figure 2) were exposed to X-ray at a single dose of 20 Gy. Next, we recorded time course changes of X-ray-induced mechanical, heat, and cold allodynia. As shown in Figure 1(c), irradiated mice showed reduced mechanical threshold one day after X-ray treatment ($t = 2.224$, $p = 0.043$). Mechanical allodynia peaked 11 days after X-ray treatment (Figure 1(c); $t = 8.951$, $p < 0.001$) and remained constant until day 28 (Figure 1(c); $t = 3.065$, $p = 0.008$).

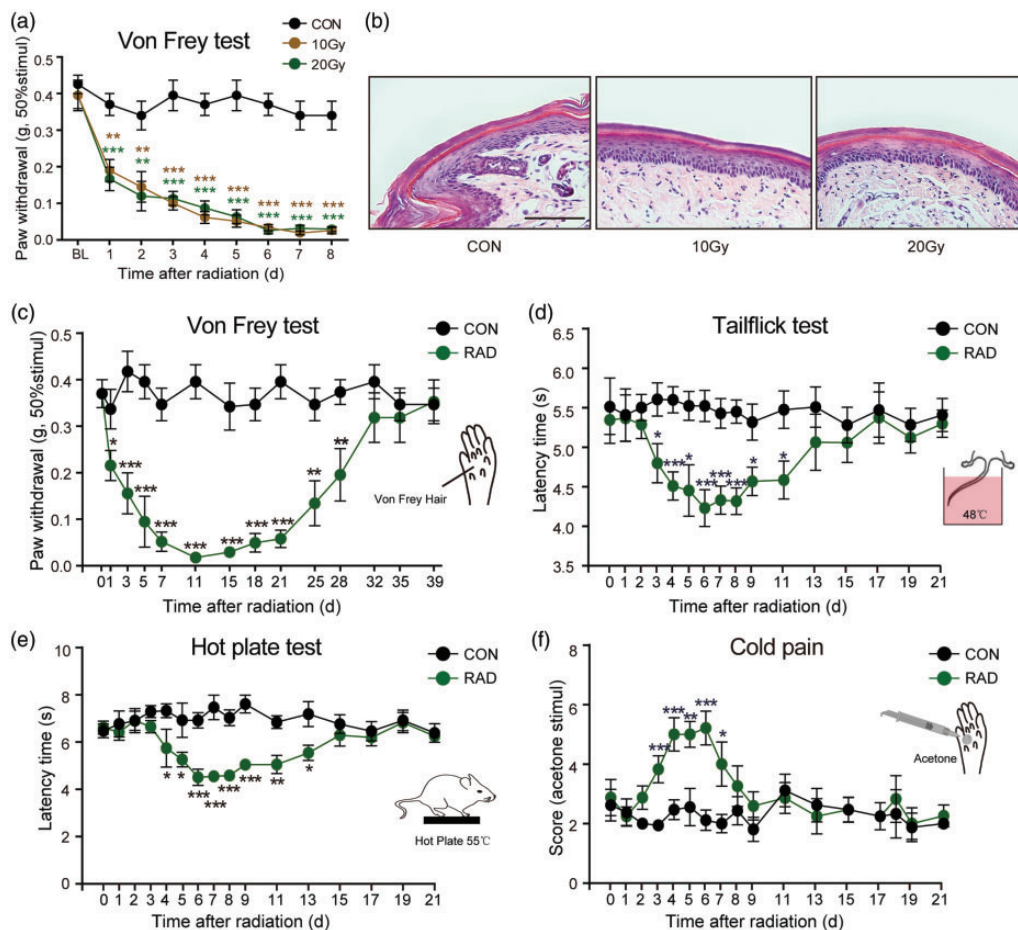


Figure 1. Ionizing radiation-induced pain-like behaviors in mice. (a) A single dose of X-ray (10 Gy or 20 Gy) exposing to right hind limb of induced a time-dependent mechanical allodynia. Data are expressed as mean \pm S.E.M. $**p < 0.01$, $***p < 0.001$, when compared to control mice. $n = 8$ mice per group. (b) The morphology of right hind paw skin was not affected at day 14 after a single X-ray treatment using H&E staining. The hind limbs and tail of mice were exposed to a single dose of 20 Gy X-ray. X-ray induced a time-dependent mechanical (c), heat (d and e), and cold (f) allodynia. Data are expressed as mean \pm S.E.M. $*p < 0.05$, $**p < 0.01$, $***p < 0.001$, when compared to control mice at the same time point ($n = 7-9$ mice). One-way analysis of variance followed by Bonferroni's post hoc test.

Heat allodynia was measured by tail-flick test and hot-plate test. As shown in Figure 1(d), the latency of tail-flick test at 48°C was significantly decreased at day 3 (5.58 ± 0.21 s in control group vs. 4.77 ± 0.25 s in radiation group, $p=0.02$), and persisted until day 11 (5.52 ± 0.24 s in control group vs. 4.73 ± 0.24 s in radiation group, $p=0.03$) after 20 Gy X-ray treatment. Similarly, the hot-plate latency was decreased at day 4 (Figure 1(e); 7.41 ± 0.30 s in control group vs. 5.83 ± 0.80 s in radiation group) and remained constant until day 13 (Figure 1(e); 7.27 ± 0.53 s in control group vs. 5.63 ± 0.33 s in radiation group). The latency was minimum at day 6 in hot-plate test and tail-flick test.

The cold pain was assessed by measuring the response to acetone-evoked evaporative cooling. The increased score was observed at day 3 (Figure 1(f); 1.94 ± 0.16 in control group vs. 3.83 ± 0.46 in radiation group, $p < 0.001$), and persisted until day 7 (Figure 1(f); 2.12 ± 0.34 in control group vs. 5.21 ± 0.57 in radiation group, $p < 0.001$) after X-ray treatment. The score of cold stimulus was maximal at day 6 (Figure 1(f); 2.00 ± 0.31 in control group vs. 4.00 ± 0.74 in radiation group, $p = 0.01$).

TRPA1 and TRPV1 are increased in DRGs after X-ray treatment

Given that the important roles of ion channels in neuropathic pain, we determined the mRNAs of a series of ion channels in DRG, 14 days after X-ray treatment. TRPV1 mRNA in DRG increased 1.6-fold in 10 Gy group (Figure 2(a); $F(2, 9) = 16.87$, $p = 0.04$) and 2.1-fold in 20 Gy group (Figure 2(a); $F(2, 9) = 16.87$, $p = 0.001$). Similarly, the mRNA of TRPV1 in DRG

increased about 2.6-fold both in 10 Gy and 20 Gy X-ray-treated mice. However, no significant change in expression of TRPV4, TRPM8, NaV1.7, or NaV1.8 mRNAs in DRG was observed after X-ray treatment (Figure 2(c) to (f)). These results indicated that TRPA1 and TRPV1 were involved in X-ray-induced allodynia.

X-ray induces oxidative stress in skin and DRG

Several studies reported that TRP channels, including TRPA1 and TRPV1, could be activated under oxidative stress condition. Indicators for oxidative stress were determined 14 days after IR treatment using real-time PCR method. Increased levels of iNOS mRNA were detected in hind paw skin (Figure 3(a); $F(2, 9) = 5.064$, $p < 0.05$) and DRG (L2–L5) (Figure 3(b); $F(2, 9) = 8.736$, $p < 0.05$) after 10 Gy or 20 Gy X-ray treatment, compared to control mice. In contrast, SOD mRNA was markedly decreased in hind paw skin (Figure 3(c); $F(2, 9) = 14.296$, $p < 0.05$) and DRG (L2–L5) (Figure 3(d); $F(2, 8) = 9.192$, $p < 0.05$) of mice treated with X-ray. CAT mRNA decreased in hind paw skin (Figure 3(e); $F(2, 9) = 14.787$, $p < 0.05$) but not in DRG in X-ray-treated mice compared to control mice. These data indicated that X-ray could result in oxidative stress, which may contribute for TRP channels activation in X-ray-induced allodynia.

Time course of TRP channels expression changes in the DRGs after X-ray treatment

To confirm the time course changes of TRP channels in DRG, we detected TRPA1, TRPV1, and TRPV4 levels in DRG using PCR and Western blot. There was no

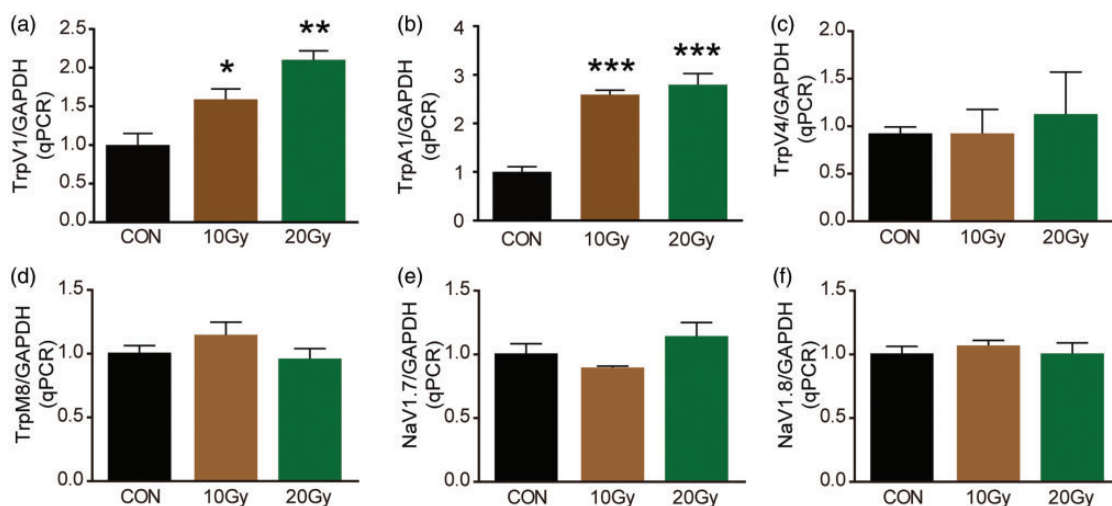


Figure 2. mRNA of ion channels was determined by qPCR. TrpA1 (a), TrpV1 (b), TrpV4 (c), TrpM8 (d), NaV1.7 (e), and NaV1.8 (f) mRNA in DRG was detected by qPCR at day 14 after a single dose of 10 Gy or 20 Gy radiation treatment. Data are expressed as mean \pm S.E.M. * $p < 0.05$, ** $p < 0.01$, *** $p < 0.001$, when compared to control mice ($n = 4$ mice). One-way analysis of variance followed by Bonferroni's post hoc test.

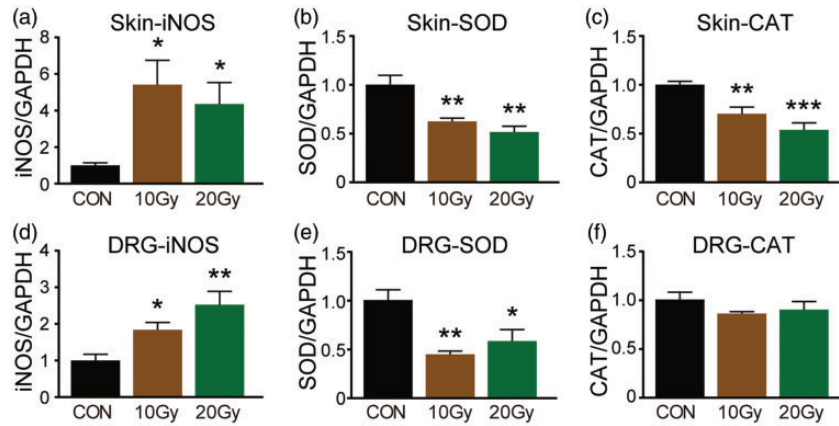


Figure 3. mRNAs of oxidative stress indicators were determined by qPCR. iNOS (a and b), SOD (c and d), CAT (e and f) mRNA in hind paw skin, and DRG was detected by qPCR at day 14 after a single dose of 10 Gy or 20 Gy radiation treatment. Data are expressed as mean \pm S.E.M. * $p < 0.05$, ** $p < 0.01$, *** $p < 0.001$, when compared to control mice ($n = 4$ mice). One-way analysis of variance followed by Bonferroni's post hoc test.

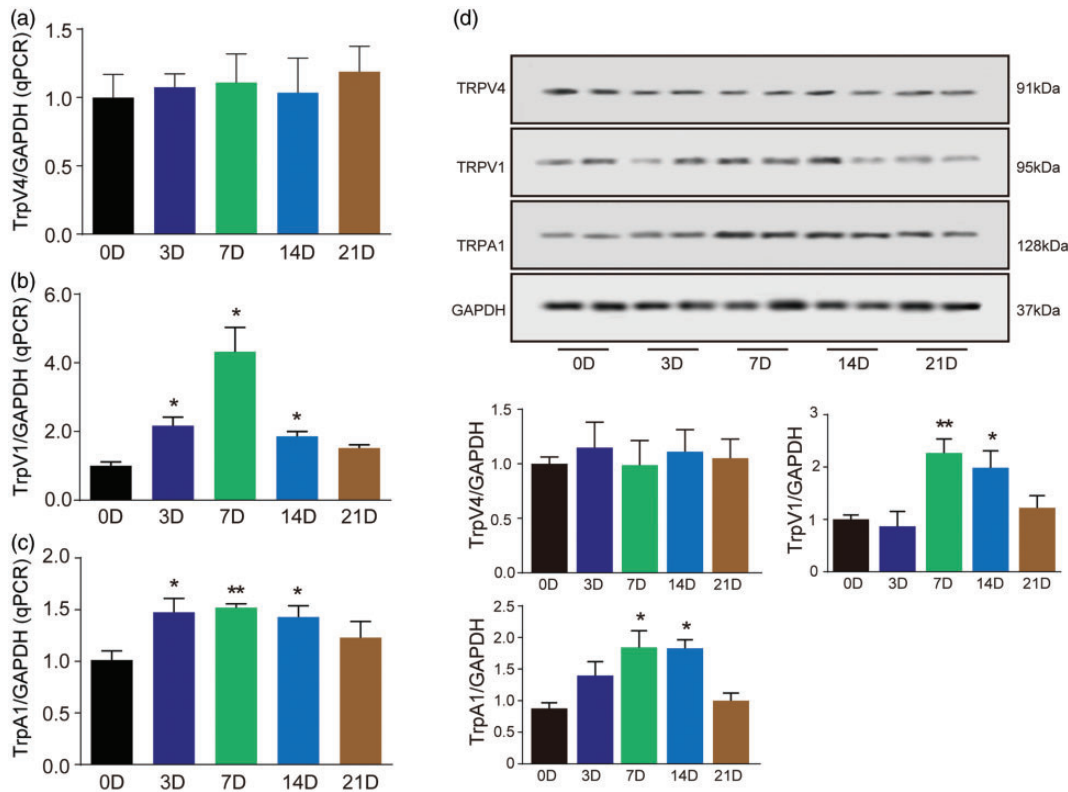


Figure 4. Time course changes of TRPA1, TRPV1, and TRPV4 in DRG after X-ray treatment. TRPV4 mRNA had no change after X-ray treatment in DRG (a). TRPV1 and TRPA1 mRNA increased at days 3, 7, and 14 in DRG (b and c). The representative Western blot images are shown in (d). Data are expressed as mean \pm S.E.M. * $p < 0.05$, ** $p < 0.01$, when compared to control mice ($n = 4$ mice). One-way analysis of variance followed by Bonferroni's post hoc test.

significant change in the expression of TRPV4 mRNA and protein in DRG at any time point from day 3 to day 21 after radiation compared with control mice (Figure 4 (a)). TRPV1 mRNA increased 2.1-fold at day 3 (Figure 4(b); $F(4, 14) = 4.39$, $p = 0.01$), 4.3-fold at day 7 (Figure

4(b); $F(4, 14) = 4.39$, $p = 0.01$) and 1.9-fold at day 14 (Figure 4(b); $F(4, 14) = 4.39$, $p = 0.008$) after X-ray treatment in DRG. Western blot analysis showed that TRPV1 was significantly increased at days 7 and 14 after radiation (Figure 4(d); $F(4, 14) = 5.752$, $p < 0.05$).

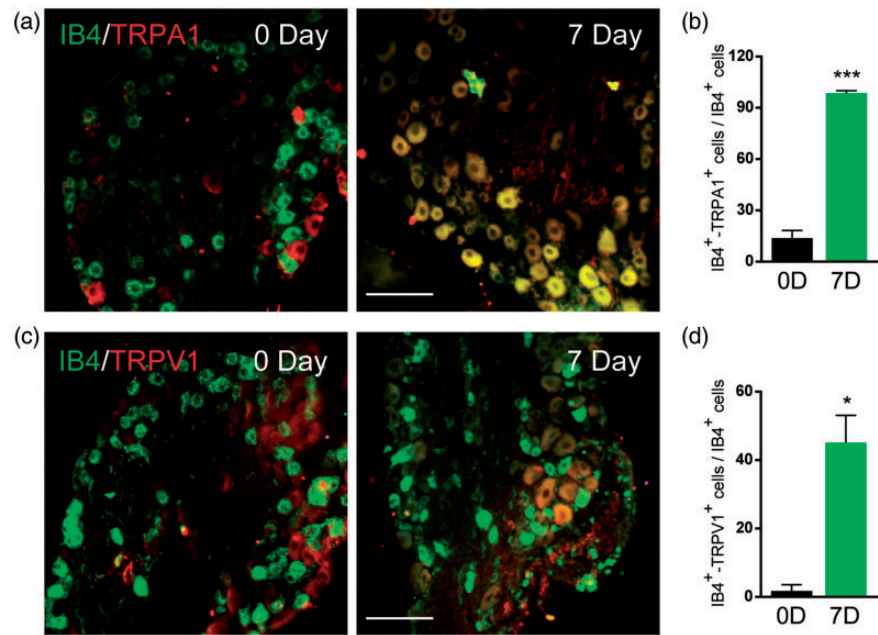


Figure 5. The co-localization of TRPA1/IB4 or TRPV1/IB4 using IHC method in DRG. IHC images showed that co-localization of TRPA1/IB4 (a) and TRPV1/IB4 (b) was significantly increased at day 7 after X-ray treatment. (c) Proportion analysis of TRPA1⁺/IB4⁺ and TRPV1⁺/IB4⁺ cells in DRG. Data are expressed as mean ± S.E.M. * $p < 0.05$, *** $p < 0.001$, when compared to control mice ($n = 4$ mice). One-way analysis of variance followed by Bonferroni's post hoc test.

TRPA1 mRNA was significantly increased at days 3, 7, and 14 after radiation (Figure 4(c); $F(4, 16) = 3.851$, $p < 0.05$). Western blot analysis showed that TRPA1 was significantly increased at days 7 and 14 after radiation (Figure 4(d); $F(4, 15) = 6.466$, $p < 0.05$). These data confirmed that TRPA1 and TRPV1, but not TRPV4, were involved in X-ray-induced allodynia.

Cellular distribution of TRPA1 and TRPV1 in the DRGs after X-ray treatment

Functional TRPA1 in DRG is primarily in the IB4-positive, calcitonin gene-related peptide (CGRP)-negative subpopulation of small lumbar DRG neurons from mouse and rat. Consistent with the Western blot results, immunohistochemical (IHC) analysis showed an increase in the expression of TRPA1 and TRPV1 at day 7 after radiation treatment. In control mice, TRPA1-positive staining was little co-localization to small DRG neurons (IB4-positive). Interestingly, IHC analysis showed that TRPA1-positive staining was primarily localized in IB4-positive DRG neurons at day 7 (Figure 5(a)). The co-localization of TRPV1 staining and IB4-positive cells was little in control mice. TRPV1 was mainly localized in IB4-positive DRG neurons at day 7 after radiation treatment (Figure 5(c)). These data indicated that TRPA1 and TRPV1 increased in small neurons contributed for X-ray-induced allodynia.

TRPA1 and TRPV1 antagonists decreased mechanical and heat allodynia induced by X-ray

Next, when the mechanical and thermal allodynia had been already established, we investigated whether TRPA1 and TRPV1 antagonists could attenuate X-ray-induced allodynia. At day 5 after radiation, spinal i.t. administration (lumbar L5–L6) of TRPA1 selective antagonist HC-030031 (10 μ g) or TRPV1 antagonist capsazepine (10 μ g) completely reverted mechanical hyperalgesia 5 h after injection (Figure 6(a); $F(3, 24) = 3.431$, $p = 0.03$ in HC-030031 group, $p = 0.01$ in capsazepine group, compared with radiation-treated mice), but this effect disappeared 12 h after HC-030031 or capsazepine injection (Figure 6(a)). The second spinal i.t. administration of HC-030031 and capsazepine was performed at day 12 after radiation. Significant mechanical threshold reduction was observed from 5 h (Figure 6(a); $F(3, 24) = 8.236$, $p = 0.001$ in HC-030031 group, $p < 0.001$ in capsazepine group, compared with X-ray-treated mice) to 12 h (Figure 6(a); $F(3, 24) = 9.103$, $p = 0.008$ in HC-030031 group, $p < 0.001$ in capsazepine group, compared with X-ray-treated mice) after HC-030031 treatment. In addition, the area under curve (AUC) within 24 h for HC-030031 and capsazepine was analyzed. The AUC for HC-030031 and capsazepine was significantly increased both after first and second i.t. injection in mechanical and heat allodynia tests (Figure 6 (b); Von Frey test, first injection, $F(3, 24) = 11.078$,

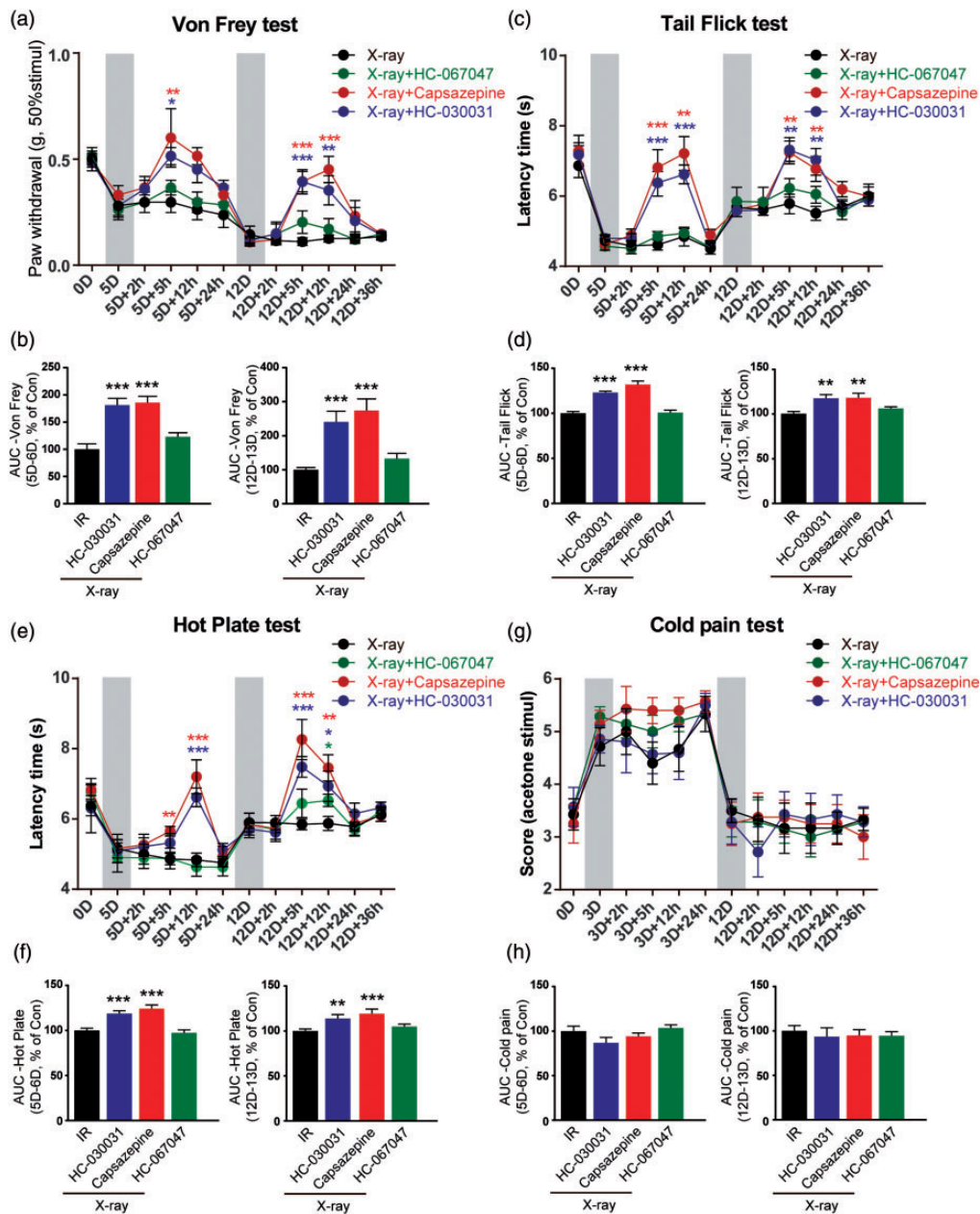


Figure 6. The effects of TRP channels antagonists on pain-like behaviors after X-ray treatment. (a) Mechanical allodynia after introtheal (i.t.) HC-030031 (10 μ g)/capsazepine (10 μ g)/HC-067047 (10 μ g) injection was assessed by Von Frey test. Heat allodynia after HC-030031/capsazepine/HC-067047 injection was assessed by tail-flick test (c) and hot-plate test (e). (g) Cold pain after HC-030031/capsazepine/HC-067047 injection was assessed by acetone test. The mechanical, heat, and cold allodynia AUC of first and second i.t. injection within 24 h is shown in (b, d, f, and h). Data are expressed as mean \pm S.E.M. * p < 0.05, ** p < 0.01, *** p < 0.001, **** p < 0.0001, when compared to IR-treated mice at the same time point (n = 7 mice). One-way analysis of variance followed by Bonferroni's post hoc test. HC-030031, TRPA1 antagonist; capsazepine, TRPV1 antagonist; HC-067047, TRPV4 antagonist.

second injection, $F(3, 24) = 10.220$; Figure 6(d), tail-flick test, first injection, $F(3, 24) = 32.484$, second injection, $F(3, 24) = 7.522$; Figure 6(f), hot-plate test, first injection, $F(3, 24) = 17.092$, second injection, $F(3, 24) = 15.816$). However, HC-030031 and capsazepine had no effect on cold pain both at day 5 and day 12 after radiation treatment (Figure 6(g) and (h)). On the other hand, HC-

067047, a TRPV4 inhibitor, had no effects on all behavioral tests, including Von Frey, tail-flick, hot-plate, and cold pain test in X-ray-treated mice (Figure 6(a), (c), (e), and (g)). In order to prove that there is no problem with the operation for HC-067047 administration, we observed the effect of HC-067047 on formalin pain. HC-067047 reduced the licking and flinching behaviors

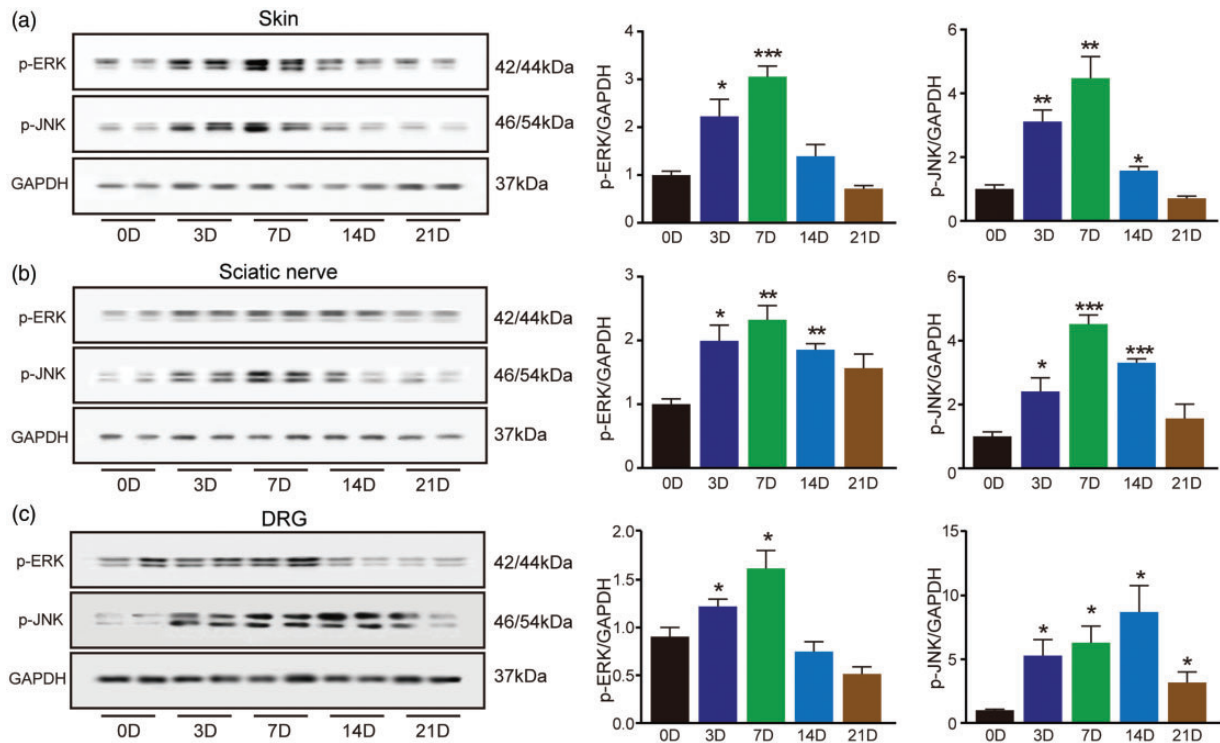


Figure 7. Time course changes of MAPK pathway in skin, sciatic nerve (SN), and DRG. The phosphorylation of ERK and JNK in skin (a), SN (b), and DRG (c) was determined by Western blot. Data are expressed as mean \pm S.E.M. * $p < 0.05$, ** $p < 0.01$, *** $p < 0.001$, when compared to control mice ($n = 4$ mice). One-way analysis of variance followed by Bonferroni's post hoc test.

after 5% formalin injection in hind paw both in phase I (0–10 min) and in phase II (10–45 min). These data are shown in Supplementary Figure 3. Our findings suggested that TRPA1 and TRPV1 contributed for mechanical and heat allodynia induced by X-ray, but TRPV4 was not involved in X-ray-induced allodynia.

Mitogen-activated protein kinase pathways was activated in pain neural pathway after X-ray treatment

TRP channels activation mediates Ca^{2+} -influx, which can activate downstream mitogen-activated protein kinase (MAPK) pathway. Activation of MAP kinases, including ERK and JNK, contributes to sensory transmission, including chemotherapy-induced peripheral neuropathic pain (CIPNP) and itch. The phosphorylation of ERK and JNK was measured by Western blot in skin, SN, and DRG. The results showed the expressions of pERK (Figure 7(a); $F(4, 13) = 18$, $p = 0.006$) and pJNK (Figure 7(a); $F(4, 14) = 17.028$, $p = 0.003$) were increased in the skin at day 3. The maximal phosphorylation degree of ERK (Figure 7(a); $F(4, 13) = 18$, $p < 0.001$) and JNK (Figure 7(a); $F(4, 14) = 17.028$, $p < 0.001$) in hind paw skin was at day 7 after radiation

treatment. Similar results were observed in the SN and DRG tissues except the change of pJNK in DRG. pJNK was increased at day 3 (Figure 7(c); $F(4, 14) = 5.825$, $p = 0.02$) and persisted until day 21 after radiation treatment. And the maximal phosphorylation of JNK in DRG was at day 14 (Figure 7(c); $F(4, 14) = 5.825$, $p = 0.001$).

Discussion

Millions of cancer patients undergo radiation therapy for treating and destroying tumor cell growths within normal cell environmental conditions. X-ray radiation can not only have positive therapeutic effects on cancer cells but also have post-detrimental effects on surrounding normal tissues.^{27,28} Since the skin is a biological defense barrier for any irradiated area, X-ray treatment can result in a variety of skin reactions and contributes to pain, itching, and burning.²⁹ X-ray-induced skin changes can affect the quality of life. Pain is unavoidable adverse event among head and neck cancer patients who are undergoing radiotherapy.²⁹ Radiation-induced pain is a late radiation-related injury, and the incidence rate is about 31% among cancer survivors treated with radiotherapy.³⁰ However,

the mechanism of X-ray-induced pain is seldom studied. Here, in a mouse model of X-ray-induced allodynia, we showed that, nociceptor TRPA1 and TRPV1 but not TRPV4 contributed to mechanical and heat allodynia induced by X-ray.

As spontaneous pain is commonly present at the site of skin exposed to X-ray, spontaneous pain-related behaviors should be simulated in the model of X-ray-related pain studies.³¹ In this study, mechanical allodynia tested by Von Frey peaked 11 days after IR exposure, to decline to normal 31 days after X-ray exposure. Heat allodynia analyzed by tail-flick and hot-plate test peaked six days after X-ray exposure and was absent two weeks later. Cold allodynia appeared at day 3, reached peak at day 5, and disappeared at day 8. By comparison, the duration of acetone-induced cold allodynia was shorter than mechanical and heat allodynia in X-ray-treated mice. In addition, there was no significant change in skin histomorphology after 10 Gy or 20 Gy radiation treatment. This result eliminated secondary pain that was associated with ulceration and abscess of skin, which can be induced by X-ray treatment.³² Thus, the current mouse model seems to appropriately recapitulate the pain-related behaviors, which are caused by radiation directly in preclinical research.

TRPA1 mRNA and protein were increased in DRG (L2–L5) after X-ray exposure. These data indicated that TRPA1 was required in X-ray-induced mechanical and heat allodynia. This conclusion was supported by the pharmacological findings. When the mechanical and heat allodynia had been already established, HC-030031, a TRPA1 antagonist, reversed pain-related behaviors after i.t. injection. Although HC-030031 reversed painful behaviors completely, the duration of maintenance was short, and the phenomenon is possibly to the short half-life of HC-030031.^{33,34}

Several studies reported that TRPV1 was increased after ultraviolet (UV) irradiation.^{35,36} A clinical investigation reported SB-705498, a TRPV1 antagonist, increased heat pain tolerance at the site of UVB exposure.³⁷ However, information about the roles of TRPV1 in X-ray-induced pain has been rarely collected. TRPV1 is located on a large subset of nociceptors and plays key roles in sensory transduction. TRPV1 can be activated in several ways, including by exogenous vanilloid chemicals (e.g., capsaicin),^{6,38} heat greater than 42°C,³⁹ and diverse endogenous lipid signals associated with inflammation.⁴⁰ In this study, TRPV1 mRNA and protein were increased in DRG after IR treatment. Also, TRPV1 antagonist capsazepine could relieve mechanical and thermal allodynia. These data suggested that TRPV1 also contributed to X-ray-induced allodynia. In addition, we observed a special phenomenon: TRPA1 and TRPV1 antagonist could not attenuate cold pain induced by X-ray. Although studies have found that responses to cold

require TRPA1,⁴¹ and blocking of TRPA1 can attenuate in oxaliplatin-induced pain and cancer pain models.^{26,42} Our finding indicates that there are unknown mechanisms underlying the cold pain induced by X-ray. It is reported that TRPV4 can be activated under the exposure of UV or γ -ray radiation.^{43,44} However, we found that X-ray had no effect on TRPV4, and blocking of TRPV4 had no effect on painful behaviors induced by X-ray. These results suggest that TRPV4 action may be selective among different types of rays.

Interestingly, IHC results showed that almost all of TRPA1⁺ cells co-localized with IB4⁺ small cells in DRG at day 7 after X-ray treatment. Studies find that very few large-diameter neurons from any species have response to TRPA1 agonist.⁴⁵ IB4-positive cutaneous afferents are critical for mechanical stimuli transduction. In addition, IB4-positive neurons become more sensitive to mechanical stimuli after tissue injury.^{46,47} Marie reported that functional TRPA1 in DRG is primarily in the IB4-positive, CGRP-negative subpopulation of small lumbar DRG neurons from mouse and rat.^{48–50} The present study indicated that TRPA1 expressing in non-peptidergic small neurons in DRG played a key role in pain signals transduction in X-ray-treated mice.

According to the temporary effect of HC-030031, we speculate that endogenous substances produced after X-ray treatment are required to activate TRPA1 in order to maintain the pain-like behaviors. Several preclinical studies and clinical investigations have shown that reactive oxygen species (ROS) and RNS are the main sources of damage to normal tissues, including lung, intestines, and skin, after exposure to X-ray.⁵¹ Given that ROS and the byproducts, including the RNS and RCS, are among the most active endogenous activators of TRPA1,^{52,53} we consider that oxidative stress induced by X-ray contributes to TRPA1 activation in the prolonged painful hypersensitivity. iNOS, a marker of oxidative stress, was increased in hind paw skin seven days after radiation when the mechanical and heat allodynia existed. In contrast, SOD and GSH, 2 antioxidant factors, were decreased in hind paw skin. Several studies reported that ROS scavengers, including metformin, 5-methoxytryptamine- α -lipoic acid, and resveratrol, significantly attenuated ROS production and protected normal tissue function from X-ray exposure.^{54–56} In addition, several studies reported that α -lipoic acid, an antioxidant, could attenuate pain-like responses by inhibiting TRPA1 in chemotherapy-induced pain and cancer pain models.^{26,57} However, the underlying mechanisms by which substance of oxidative stress initiates the pain signals in X-ray-induced pain are still needed further research. In addition, TRP channels activation can induce Ca²⁺ influx, then activate the downstream MAPK pathway. MAPK, including ERK, JNK, and p38, is required to maintain allodynia under

inflammatory pain,⁵⁸ and inhibition of MAPK could reduce neuropathic pain.⁵⁹ In this study, both of pJNK and pERK were significantly increased in skin, SN, and DRG. These data suggested that MAPK pathway was involved in X-ray-induced allodynia. However, it still needs to study that whether inhibition of MAPK pathway can attenuate allodynia induced by X-ray.

In summary, our work confirmed that TRPV1 and TRPA1 contributed to X-ray-induced allodynia. The experimental data indicated that blocking of TRPV1 and TRPA1 was beneficial for relieving allodynia induced by X-ray. Although X-ray treatment resulted in oxidative stress in our study. Antioxidation helps to alleviate pain in several animal models, but at the same time, antioxidation may reduce the sensitivity of tumors to radiotherapy and reduce the therapeutic effect finally. However, deletion of TRPV1 or TRPA1 does not affect tumor growth.²⁶ So, TRPV1 and TRPA1 antagonists appear to be the suitable prevention strategies for X-ray-induced allodynia in clinical practice.

Author's Note

Xu Jian-Hao is also affiliated to Department of Pathology, Kunshan First People's Hospital Affiliated to Jiangsu University, Kunshan, China.

Declaration of Conflicting Interests

The author(s) declared no potential conflicts of interest with respect to the research, authorship, and/or publication of this article.

Funding

The author(s) disclosed receipt of the following financial support for the research, authorship, and/or publication of this article: This work was supported by the National Science Foundation of China (81601098, 81603181, and 81300968), Natural Science Foundation of Jiangsu Province, China (BK20170004 and 2015-JY-029), Suzhou Science Foundation (SYS201344), and Natural Science Foundation of Jiangsu Higher Education institutions (14KJB320011).

ORCID iD

Su Cun-Jin  <https://orcid.org/0000-0003-3728-3377>

References

- Loi M, Desideri I, Greto D, Mangoni M, Sottili M, Meattini I, Becherini C, Terziani F, Delli Paoli C, Olmetto E, Bonomo P and Livi L. Radiotherapy in the age of cancer immunology: current concepts and future developments. *Crit Rev Oncol Hematol* 2017; 112: 1–10.
- He MY, Rancoule C, Rehailla-Blanchard A, Espenel S, Trone J-C, Bernichon E, Guillaume E, Vallard A and Magné N. Radiotherapy in triple-negative breast cancer: current situation and upcoming strategies. *Crit Rev Oncol Hematol* 2018; 131: 96–101.
- Badiyan SN, Molitoris JK, Chuong MD, Regine WF and Kaiser A. The role of radiation therapy for pancreatic cancer in the adjuvant and neoadjuvant settings. *Surg Oncol Clin N Am* 2017; 26: 431–453.
- Christensen DM, Iddins CJ, Parrillo SJ, Glassman ES and Goans RE. Management of ionizing radiation injuries and illnesses, part 4: acute radiation syndrome. *J Am Osteopath Assoc* 2014; 114: 702–711.
- Beach TA, Groves AM, Williams JP and Finkelstein JN. Modeling radiation-induced lung injury: lessons learned from whole thorax irradiation. *Int J Radiat Biol*. Epub ahead of print 25 October 2018. DOI: 10.1080/09553002.2018.1532619.
- Soriano JL, Calpena AC, Souto EB and Clares B. Therapy for prevention and treatment of skin ionizing radiation damage: a review. *Int J Radiat Biol*. Epub ahead of print 20 December 2018. DOI: 10.1080/09553002.2019.1562254.
- Song J, Zhang H, Wang Z, Xu W, Zhong L, Cao J, Yang J, Tian Y, Yu D, Ji J, Cao J and Zhang S. The role of FABP5 in radiation-induced human skin fibrosis. *Radiat Res* 2018; 189: 177–186.
- Lee J, Park W, Choi DH, Huh SJ, Kim IR, Kang D and Cho J. Patient-reported symptoms of radiation dermatitis during breast cancer radiotherapy: a pilot study. *Qual Life Res* 2017; 26: 1713–1719.
- Mulliez T, Veldeman L, van Greveling A, Speleers B, Sadeghi S, Berwouts D, Decoster F, Vercauteren T, De Gerssem W, Van den Broecke R and De Neve W. Hypofractionated whole breast irradiation for patients with large breasts: a randomized trial comparing prone and supine positions. *Radiother Oncol* 2013; 108: 203–208.
- Salvo N, Barnes E, van Draanen J, Stacey E, Mitera G, Breen D, Giotis A, Czarnota G, Pang J and De Angelis C. Prophylaxis and management of acute radiation-induced skin reactions: a systematic review of the literature. *Curr Oncol* 2010; 17: 94–112.
- Yee C, Wang K, Asthana R, Drost L, Lam H, Lee J, Vesprini D, Leung E, DeAngelis C and Chow E. Radiation-induced skin toxicity in breast cancer patients: a systematic review of randomized trials. *Clin Breast Cancer* 2018; 18: e825–e840.
- Sisignano M, Angioni C, Park CK, Meyer Dos Santos S, Jordan H, Kuzikov M, Liu D, Zinn S, Hohman SW, Schreiber Y, Zimmer B, Schmidt M, Lu R, Suo J, Zhang DD, Schafer SM, Hofmann M, Yekkirala AS, de Bruin N, Parnham MJ, Woolf CJ, Ji RR, Scholich K and Geisslinger G. Targeting CYP2J to reduce paclitaxel-induced peripheral neuropathic pain. *Proc Natl Acad Sci USA* 2016; 113: 12544–12549.
- Hershman DL, Lacchetti C, Dworkin RH, Lavoie Smith EM, Bleeker J, Cavaletti G, Chauhan C, Gavin P, Lavino A, Lustberg MB, Paice J, Schneider B, Smith ML, Smith T, Terstriep S, Wagner-Johnston N, Bak K, Loprinzi CL and American Society of Clinical Oncology. Prevention and management of chemotherapy-induced peripheral neuropathy in survivors of adult cancers: American

- Society of Clinical Oncology clinical practice guideline. *JCO* 2014; 32: 1941–1967.
14. Moran MM and Szallasi A. Targeting nociceptive transient receptor potential channels to treat chronic pain: current state of the field. *Br J Pharmacol* 2018; 175: 2185–2203.
 15. Balemans D, Boeckstaens GE, Talavera K and Wouters MM. Transient receptor potential ion channel function in sensory transduction and cellular signaling cascades underlying visceral hypersensitivity. *Am J Physiol Gastrointest Liver Physiol* 2017; 312: G635–G648.
 16. Masuoka T, Kudo M, Yamashita Y, Yoshida J, Imaizumi N, Muramatsu I, Nishio M and Ishibashi T. TRPA1 channels modify TRPV1-mediated current responses in dorsal root ganglion neurons. *Front Physiol* 2017; 8: 272.
 17. Kozai D, Ogawa N and Mori Y. Redox regulation of transient receptor potential channels. *Antioxid Redox Signal* 2014; 21: 971–986.
 18. Shimizu S, Takahashi N and Mori Y. TRPs as chemosensors (ROS, RNS, RCS, gasotransmitters). *Handb Exp Pharmacol* 2014; 223: 767–794.
 19. Sagalajev B, Wei H, Chen Z, Albayrak I, Koivisto A and Pertovaara A. Oxidative stress in the amygdala contributes to neuropathic pain. *Neuroscience* 2018; 387: 92–103.
 20. Aubdool AA, Kodji X, Abdul-Kader N, Heads R, Fernandes ES, Bevan S and Brain SD. TRPA1 activation leads to neurogenic vasodilatation: involvement of reactive oxygen nitrogen species in addition to CGRP and NO. *Br J Pharmacol* 2016; 173: 2419–2433.
 21. Chakrabarti S, Pattison LA, Singhal K, Hockley JRF, Callejo G and Smith E. Acute inflammation sensitizes knee-innervating sensory neurons and decreases mouse digging behavior in a TRPV1-dependent manner. *Neuropharmacology* 2018; 143: 49–62.
 22. Boyette-Davis JA, Walters ET and Dougherty PM. Mechanisms involved in the development of chemotherapy-induced neuropathy. *Pain Manag* 2015; 5: 285–296.
 23. Sondermann JR, Barry AM, Jahn O, Michel N, Abdelaziz R, Kugler S, Gomez-Varela D and Schmidt M. Vti1b promotes TRPV1 sensitization during inflammatory pain. *Pain* 2019; 160: 508–527.
 24. Hylden JL and Wilcox GL. Intrathecal morphine in mice: a new technique. *Eur J Pharmacol* 1980; 67: 313–316.
 25. Xu ZZ, Zhang L, Liu T, Park JY, Berta T, Yang R, Serhan CN and Ji RR. Resolvins RvE1 and RvD1 attenuate inflammatory pain via central and peripheral actions. *Nat Med* 2010; 16: 592–597, 1p following 597.
 26. Antoniazzi CTD, Nassini R, Rigo FK, Milioli AM, Bellinaso F, Camponogara C, Silva CR, de Almeida AS, Rossato MF, De Logu F, Oliveira SM, Cunha TM, Geppetti P, Ferreira J and Trevisan G. Transient receptor potential ankyrin 1 (TRPA1) plays a critical role in a mouse model of cancer pain. *Int J Cancer* 2019; 144: 355–365.
 27. Mettler FA Jr and Voelz GL. Major radiation exposure—what to expect and how to respond. *N Engl J Med* 2002; 346: 1554–1561.
 28. Pathak R, Shah SK and Hauer-Jensen M. Therapeutic potential of natural plant products and their metabolites in preventing radiation enteropathy resulting from abdominal or pelvic irradiation. *Int J Radiat Biol* 2019; 95: 493–505.
 29. Gourd E. Pregabalin alleviates radiotherapy-related neuropathic pain. *Lancet Oncol* 2019; 20: e12.
 30. Manas A, Monroy JL, Ramos AA, Cano C, Lopez GV, Masramon X, Perez M. and Group Tcs Prevalence of neuropathic pain in radiotherapy oncology units. *Int J Radiat Oncol Biol Phys* 2011; 81: 511–520.
 31. Jaggi AS, Jain V and Singh N. Animal models of neuropathic pain. *Fundam Clin Pharmacol* 2011; 25: 1–28.
 32. Ryan JL. Ionizing radiation: the good, the bad, and the ugly. *J Invest Dermatol* 2012; 132: 985–993.
 33. Eid SR, Crown ED, Moore EL, Liang HA, Choong KC, Dima S and Henze DA. Kane SA and Urban MO. HC-030031, a TRPA1 selective antagonist, attenuates inflammatory- and neuropathy-induced mechanical hypersensitivity. *Mol Pain* 2008; 4: 48.
 34. Chen J, Joshi SK, DiDomenico S, Perner RJ, Mikusa JP, Gauvin DM, Segreti JA, Han P, Zhang XF, Niforatos W, Bianchi BR, Baker SJ, Zhong C, Simler GH, McDonald HA, Schmidt RG, McGaraughty SP, Chu KL, Faltynek CR, Kort ME, Reilly RM and Kym PR. Selective blockade of TRPA1 channel attenuates pathological pain without altering noxious cold sensation or body temperature regulation. *Pain* 2011; 152: 1165–1172.
 35. Kang SM, Han S, Oh JH, Lee YM, Park CH, Shin CY, Lee DH and Chung JH. A synthetic peptide blocking TRPV1 activation inhibits UV-induced skin responses. *J Dermatol Sci* 2017; 88: 126–133.
 36. Lee YM, Kang SM, Lee SR, Kong KH, Lee JY, Kim EJ and Chung JH. Inhibitory effects of TRPV1 blocker on UV-induced responses in the hairless mice. *Arch Dermatol Res* 2011; 303: 727–736.
 37. Modir JG and Wallace MS. Human experimental pain models 1: the ultraviolet light UV-B pain model. *Meth Mol Biol* 2010; 617: 159–164.
 38. Bevan S, Hothi S, Hughes G, James IF, Rang HP, Shah K, Walpole CS and Yeats JC. Capsazepine: a competitive antagonist of the sensory neurone excitant capsaicin. *Br J Pharmacol* 1992; 107: 544–552.
 39. Gavva NR, Klionsky L, Qu Y, Shi L, Tamir R, Edenson S, Zhang TJ, Viswanadhan VN, Toth A, Pearce LV, Vanderah TW, Porreca F, Blumberg PM, Lile J, Sun Y, Wild K, Louis JC and Treanor JJ. Molecular determinants of vanilloid sensitivity in TRPV1. *J Biol Chem* 2004; 279: 20283–20295.
 40. Park CK, Lu N, Xu ZZ, Liu T, Serhan CN and Ji RR. Resolving TRPV1- and TNF-alpha-mediated spinal cord synaptic plasticity and inflammatory pain with neuroprotectin D1. *J Neurosci* 2011; 31: 15072–15085.
 41. Chatzigeorgiou M, Yoo S, Watson JD, Lee W-H, Spencer WC, Kindt KS, Hwang SW, Miller Iii DM, Treinin M, Driscoll M and Schafer WR. Specific roles for DEG/ENaC and TRP channels in touch and thermosensation in *C. elegans* nociceptors. *Nat Neurosci* 2010; 13: 861–868.
 42. Nassini R, Gees M, Harrison S, De Siena G, Materazzi S, Moretto N, Failli P, Preti D, Marchetti N, Cavazzini A, Mancini F, Pedretti P, Nilius B, Patacchini R and Geppetti

- P. Oxaliplatin elicits mechanical and cold allodynia in rodents via TRPA1 receptor stimulation. *Pain* 2011; 152: 1621–1631.
43. Ohsaki A, Tanuma SI and Tsukimoto M. TRPV4 channel-regulated ATP release contributes to gamma-irradiation-induced production of IL-6 and IL-8 in epidermal keratinocytes. *Biol Pharm Bull* 2018; 41: 1620–1626.
 44. Moore C, Cevikbas F, Pasolli HA, Chen Y, Kong W, Kempkes C, Parekh P, Lee SH, Kontchou NA, Yeh I, Jokerst NM, Fuchs E, Steinhoff M and Liedtke WB. UVB radiation generates sunburn pain and affects skin by activating epidermal TRPV4 ion channels and triggering endothelin-1 signaling. *Proc Natl Acad Sci USA* 2013; 110: E3225–E3234.
 45. Barabas ME, Kossyryeva EA and Stucky CL. TRPA1 is functionally expressed primarily by IB4-binding, non-peptidergic mouse and rat sensory neurons. *PLoS One* 2012; 7: e47988.
 46. Kwan KY, Allchorne AJ, Vollrath MA, Christensen AP, Zhang DS, Woolf CJ and Corey DP. TRPA1 contributes to cold, mechanical, and chemical nociception but is not essential for hair-cell transduction. *Neuron* 2006; 50: 277–289.
 47. Drew LJ, Wood JN and Cesare P. Distinct mechanosensitive properties of capsaicin-sensitive and -insensitive sensory neurons. *J Neurosci* 2002; 22: RC228.
 48. Kim YS, Son JY, Kim TH, Paik SK, Dai Y, Noguchi K, Ahn DK and Bae YC. Expression of transient receptor potential ankyrin 1 (TRPA1) in the rat trigeminal sensory afferents and spinal dorsal horn. *J Comp Neurol* 2010; 518: 687–698.
 49. Hjerling-Leffler J, Alqatari M, Ernfors P and Koltzenburg M. Emergence of functional sensory subtypes as defined by transient receptor potential channel expression. *J Neurosci* 2007; 27: 2435–2443.
 50. Caspani O, Zurborg S, Labuz D and Heppenstall PA. The contribution of TRPM8 and TRPA1 channels to cold allodynia and neuropathic pain. *PLoS One* 2009; 4: e7383.
 51. Koerdt S, Tanner N, Rommel N, Rohleder NH, Stoeckelhuber M, Wolff KD and Kesting MR. An immunohistochemical study on the role of oxidative and nitrosative stress in irradiated skin. *Cells Tissues Organs* 2017; 203: 12–19.
 52. Taylor-Clark TE, Ghatta S, Bettner W and Udem BJ. Nitrooleic acid, an endogenous product of nitrative stress, activates nociceptive sensory nerves via the direct activation of TRPA1. *Mol Pharmacol* 2009; 75: 820–829.
 53. Suzawa S, Takahashi K, Shimada T and Ohta T. Carbonyl stress-induced 5-hydroxytryptamine secretion from RIN-14B, rat pancreatic islet tumor cells, via the activation of transient receptor potential ankyrin 1. *Brain Res Bull* 2016; 125: 181–186.
 54. Xu G, Wu H, Zhang J, Li D, Wang Y, Wang Y, Zhang H, Lu L, Li C, Huang S, Xing Y, Zhou D and Meng A. Metformin ameliorates ionizing irradiation-induced long-term hematopoietic stem cell injury in mice. *Free Radic Biol Med* 2015; 87: 15–25.
 55. Manda K, Ueno M, Moritake T and Anzai K. Alpha-Lipoic acid attenuates x-irradiation-induced oxidative stress in mice. *Cell Biol Toxicol* 2007; 23: 129–137.
 56. Ye K, Ji CB, Lu XW, Ni YH, Gao CL, Chen XH, Zhao YP, Gu GX and Guo XR. Resveratrol attenuates radiation damage in *Caenorhabditis elegans* by preventing oxidative stress. *J Radiat Res* 2010; 51: 473–479.
 57. Guo Y, Jones D, Palmer JL, Forman A, Dakhil SR, Velasco MR, Weiss M, Gilman P, Mills GM, Noga SJ, Eng C, Overman MJ and Fisch MJ. Oral alpha-lipoic acid to prevent chemotherapy-induced peripheral neuropathy: a randomized, double-blind, placebo-controlled trial. *Support Care Cancer* 2014; 22: 1223–1231.
 58. Gao YJ, Xu ZZ, Liu YC, Wen YR, Decosterd I and Ji RR. The c-Jun N-terminal kinase 1 (JNK1) in spinal astrocytes is required for the maintenance of bilateral mechanical allodynia under a persistent inflammatory pain condition. *Pain* 2010; 148: 309–319.
 59. Huang CT, Chen SH, Lin SC, Chen WT, Lue JH and Tsai YJ. Erythropoietin reduces nerve demyelination, neuropathic pain behavior and microglial MAPKs activation through erythropoietin receptors on Schwann cells in a rat model of peripheral neuropathy. *Glia* 2018; 66: 2299–2315.